Environ. Sci. Technol. **1999**, *33,* 63−73

Bacteriophage PRD1 and Silica Colloid Transport and Recovery in an Iron Oxide-Coated Sand Aquifer

JOSEPH N. RYAN,*,† MENACHEM ELIMELECH,‡ REBECCA A. ARD,† RONALD W. HARVEY,§ AND PHILIP R. JOHNSON⊥

Department of Civil, Environmental, and Architectural Engineering, Campus Box 428, University of Colorado, Boulder, Colorado 80309-0428, Department of Chemical Engineering, Environmental Engineering Program, Yale University, New Haven, Connecticut 06520, U.S. Geological Survey, Water Resources Division, 3215 Marine Street, Boulder, Colorado 80303-1066, and Department of Civil Engineering and Geological Sciences, University of Notre Dame, Notre Dame, Indiana 46556

Bacteriophage PRD1 and silica colloids were co-injected into sewage-contaminated and uncontaminated zones of an iron oxide-coated sand aquifer on Cape Cod, MA, and their transport was monitored over distances up to 6 m in three arrays. After deposition, the attached PRD1 and silica colloids were mobilized by three different chemical perturbations (elevated pH, anionic surfactant, and reductant). PRD1 and silica colloids experienced less attenuation in the contaminated zone where adsorbed organic matter and phosphate may be hindering attachment of PRD1 and silica colloids to the iron oxide coatings. The PRD1 collision efficiencies agree well with collision efficiencies predicted by assuming favorable PRD1 deposition on iron oxide coatings for which the surface area coverage was measured by microprobe analysis of sediment thin sections. ζ potentials of the PRD1, silica colloids, and aquifer grains corroborated the transport results, indicating that electrostatic forces dominated the attachment of PRD1 and silica colloids. Elevated pH was the chemical perturbation most effective at mobilizing the attached PRD1 and silica colloids. Elevated surfactant concentration mobilized the attached PRD1 and silica colloids more effectively in the contaminated zone than in the uncontaminated zone.

Introduction

The transport of pathogenic enteric viruses in groundwater is a serious threat to the safety of many drinking water supplies in the United States. To control this threat, the U.S. Environmental Protection Agency is evaluating rules that will require water utilities to disinfect groundwater unless it can be demonstrated that "natural disinfection" of viruses and other microbial pathogens occurs in an aquifer (*1, 2*). Attachment to sediments and inactivation are the two major natural disinfection processes that attenuate the transport of infective viruses in an aquifer. Our ability to predict virus transport in groundwater depends on better understanding of these processes.

Current models of virus transport in groundwater treat viruses as colloids that can "die" or be rendered inactive (*3, 4*). After accounting for virus inactivation with a temperature-dependent decay term for mobile viruses, attachment has been modeled by colloid filtration (*5*) modified to include kinetically controlled release (*6, 7*). Attachment occurs in two steps, transport and surface interaction, modeled as a collision frequency (η) and collision efficiency (α). Release is modeled as a first-order reaction incorporating the kinetics of two steps, surface interaction and diffusion away from the surface, in a release rate coefficient. The major difficulty in predicting virus attachment is obtaining values for the collision efficiency and the release rate coefficient.

Viruses and inorganic colloids respond similarly to changes in solution and surface chemistry as they migrate through porous media (*8, 9*). For both viruses and colloids, increases in ionic strength and bivalent cations and the presence of positively charged surfaces on aquifer grains (e.g., iron oxide, clay edges) promote attachment. Increases in pH or organic matter concentration generally inhibit virus and colloid attachment. For colloid release, these chemical perturbations have the opposite effect—high ionic strength inhibits release and high pH and organic matter promote release. The effects of these chemical perturbations on colloid transport in porous media have been firmly linked to electrostatic interactions incorporated in the Derjaguin−Landau−Verwey−Overbeek (DLVO) theory using the interaction force boundary layer model (*10, 11*). This approach typically underpredicted collision efficiencies (*12, 13*) until surface heterogeneities on the collector grains were taken into account (*14, 15*). The DLVO approach appears promising for some viruses (*16−19*), but certain nonelectrostatic forces (hydrophobic, steric) may also affect virus transport (*18, 20, 21*). In general, these nonelectrostatic forces are not significant for mineral colloids.

To test the effects of electrostatic and nonelectrostatic forces on the transport of viruses in saturated porous media, we compared the transport and recovery of a virus (bacteriophage PRD1) with silica colloids in sewage-contaminated and uncontaminated zones of an iron oxide-coated sand aquifer on Cape Cod, MA. In the past, direct comparisons of attachment and detachment of viruses, bacteria, protozoa, and polystyrene latex microspheres have been examined in this aquifer (*22−25*), but the electrostatic properties of the biocolloid, colloid, and aquifer grain surfaces were not compared. In this study, ζ potentials of the bacteriophage PRD1, silica colloids, and aquifer grains were obtained by electrokinetic measurements to compare the role of electrostatic forces in virus and colloid transport.

Materials and Methods

Site Description. The PRD1 and silica colloid injections were conducted in the surficial aquifer at the U.S. Geological Survey's Cape Cod Toxic Waste Research Site near the Massachusetts Military Reservation on Cape Cod. About 50 years of secondary sewage effluent disposal onto infiltration beds about 500 m up-gradient of the site created a ground-

* Corresponding author: Campus Box 428, University of Colorado, Boulder, CO 80309-0428 (mailing address); Engineering Center OT441, University of Colorado, Boulder, CO 80309-0428 (street address); phone: (303)492-0772; fax: (303)492-7317; e-mail: joe.ryan@colorado.edu.

† University of Colorado.

‡ Yale University.

§ U.S. Geological Survey.

⊥ University of Notre Dame.

10.1021/es980350+ CCC: $18.00
Published on Web 11/19/1998

TABLE 1. Chemistry of the Groundwater in the Unconfined Glacial Outwash Aquifer Approximately 150 m Downstream of the Sewage Infiltration Beds at the Cape Cod Site

constituent	unit	uncontaminated zone	contaminated zone	ref
pH		5.4−5.6	5.8−6.0	this study
specific conductance	μS cm^{-1}	30−40	250−330	this study
ionic strength	mM	0.5	4.0	this study
temperature	°C	15.5	15.0	this study
dissolved oxygen	mg L^{-1}	4.5−6.5	0−0.5	this study
dissolved organic carbon	mg L^{-1}	0.4−1.0	2.0−4.4	this study
MBAS[a]	mg L^{-1}	0.05	0.10	this study
Na^+	μM	250	1,900	26
K^+	μM	21	200	26
Mg^{2+}	μM	37	130	26
Ca^{2+}	μM	28	210	26
NH_4^+	μM	<1	<1	26
Mn (dissolved)	μM	0.64	15	26
Fe(II)	μM	<0.05	0.16	this study
Cl^-	μM	230	760	26
NO_3^-	μM	<10	300	26
HCO_3^-	μM	28	640	26
SO_4^{2-}	μM	85	360	26
$PO_4$3-	μM	0.74	12	26
sediment Fe(III)[b]	μmol g^{-1}	3.6 ± 0.3	4.7 ± 1.4	31
sediment phosphate	μmol g^{-1}	0.61 ± 0.09	0.58−1.5	71
sediment f_{oc}		<0.0001	0.01	56, 72

[a] MBAS, methylene blue active substances (detergents, surfactants). [b] Sediment Fe(III) is the concentration of iron extracted by a Ti(III)−citrate−EDTA−bicarbonate solution (*73*).

water contaminant plume characterized by low dissolved oxygen and elevated pH, specific conductivity, and organic carbon (*26*) (Table 1). The site has been used to study the transport of salts, metals, nutrients, detergents, microspheres, bacteria, protozoa, and viruses (*6*, *22*−*24*, *27*−*31*). Constituents injected in these previous studies were not present in the sampling arrays used in this investigation. The aquifer sediments consist of Pleistocene glacial outwash with interbedded sand and gravel layers with an effective porosity of 0.39 (*32*). The grains (average diameter 0.6 mm) consist mainly of quartz coated by clays and ferric and aluminum oxyhydroxides (*33*).

Injections. During July and August 1996, injections were made into three arrays of multilevel samplers (MLSs; 3−11, 3−12, and 4−15). Each array consisted of an injection MLS and four to six monitoring MLSs at down-gradient intervals of approximately 1 m (Figure 1). Three identical virus and colloid injections were followed by three different chemical perturbation injections (Table 2). The injections in arrays 2 and 3 were preceded by chemical perturbation injections (elevated anionic surfactant and reductant concentration) that mobilized natural colloids. For each injection, groundwater from the uncontaminated zone (6.4 and 6.7 m depths) and the contaminated zone (8.7 and 9.0 m depths) was pumped at a rate of 1.0 L min^{-1} from the injection MLS into two gas-impermeable, acid-cleaned 100 L fuel bladders (Aero Tech Lab; Ramsey, NJ). The contaminated groundwater bladder was purged and filled with nitrogen gas before filling with groundwater. After the injection constituents were added and mixed by agitation, the two 100 L injectates were simultaneously pumped back to depths of 6.4 and 8.7 m at a flow rate of about 1.0 L min^{-1}.

Sampling and Field Analysis. We sampled six depths in each of the MLSs immediately before and after the injections to measure background and initial concentrations (C_0) of each constituent. Following the injections, samples were collected daily. Samples were withdrawn at a rate of about 200 mL min^{-1} by peristaltic pumps through polyethylene and Norprene tubing. Samples were collected after purging about 100 mL of water from the MLS tubes. In the field, pH and specific conductance were measured with a combination pH electrode (Orion 8104), conductivity electrode, and combination pH/conductivity meter (Fisher Accumet 20). Dissolved oxygen was measured with 0−1 mg L^{-1} Rhodazine D and 1−12 mg L^{-1} indigo carmine test kits (CHEMetrics, Inc.). Ferrous iron was measured with a 1,10-phenanthroline 0.1−10 mg L^{-1} test kit (CHEMetrics, Inc.).

Virus. PRD1 is bacteriophage isolated from municipal sewage (*34*) that is similar in size and surface character to enteroviruses of public health concern (*35*). It is icosahedral in shape with a diameter of 62 nm. It consists of 70% protein, 15% phospholipids, and 15% DNA (*36*). Its pH_{iep} has been measured at <4.5 in a calcium phosphate buffer solution containing 10^{-4} M calcium (*7*). PRD1 inactivation in groundwater from Cape Cod and other sites at temperatures from 7 to 23 °C (*25*, *37*) has been considered negligible during field experiments of up to 14 days duration (*24*, *25*). To facilitate analysis of the total PRD1 concentration (both infective and noninfective), the PRD1 were radiolabeled with ^{32}P-phosphate following methods described previously (*17*). Both the phospholipid layer within the protein capsid and the DNA are presumed to have incorporated ^{32}P. On the basis of the optical density of the PRD1 stock and the extinction coefficient of typical proteins in virus capsids (*38*), the specific radioactivity of the labeled PRD1 was 0.022 ± 0.007 count min^{-1} per virus. Virus samples were shipped every 3 days to the USGS laboratory in Boulder, CO, mixed with scintillation cocktail (Packard Ultima Gold), and measured by liquid scintillation counting (Beckman LS3801). All ^{32}P count rates were adjusted for the background count rate (110 ± 4 counts min^{-1}) and radioactive decay. Error between replicate samples for this method was about 10%. The relative detection limit of this method was $C\ C_0^{-1} = 0.003-0.021$, depending on the ^{32}P−PRD1 C_0 value.

Silica Colloids. The silica colloids (Nissan Chemical Industries) have a density of 2.19 g mL^{-1} and a mean ($\pm\sigma$) diameter of 107 ± 21 nm determined by dynamic light scattering (Particle Sizing Systems, Model 370, Santa Barbara, CA). Silica colloid concentration was measured by ultraviolet (UV) spectrophotometry (λ = 340 nm, Milton Roy Spectronic 601) and turbidity (Hach Co. Ratio X/R). UV calibration curves (R^2 > 0.96) were measured in uncontaminated and

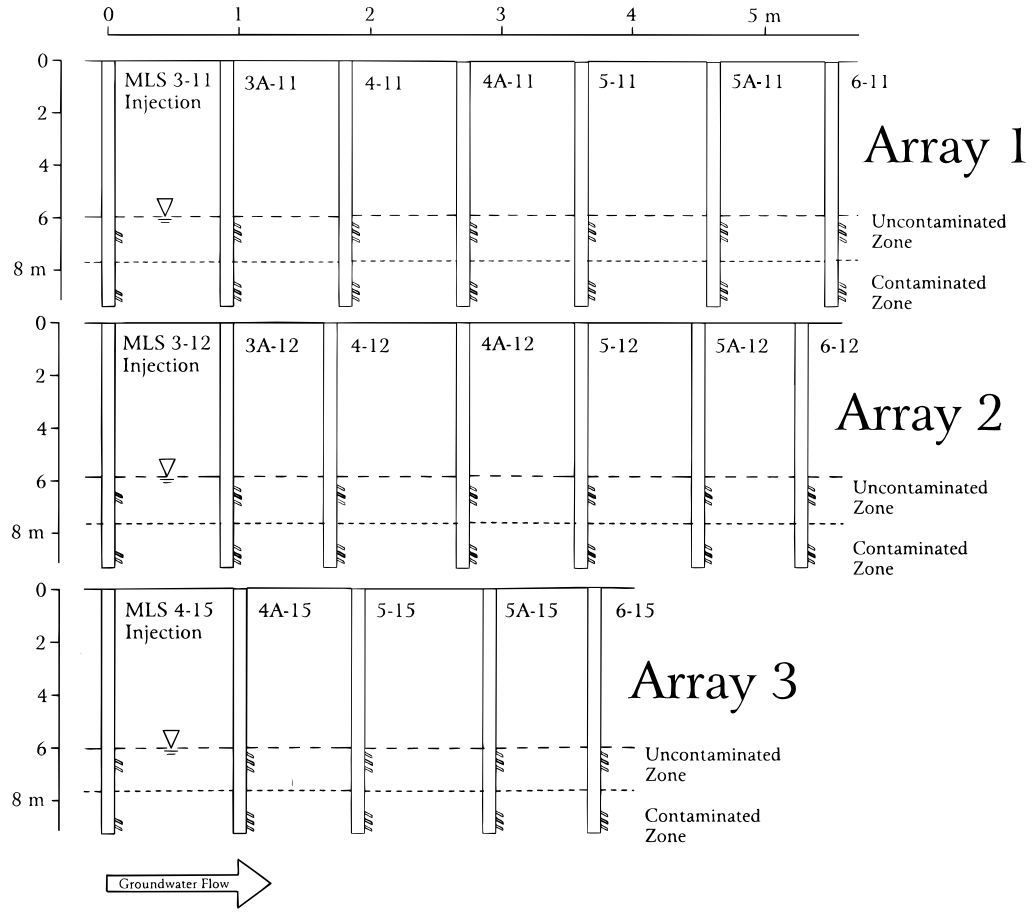

FIGURE 1. Schematic of multilevel sampler (MLS) arrays used for PRD1 and silica colloid deposition and recovery experiments. Data presented only from first MLS down-gradient of injection wells. Ports used for injection and sampling shown on MLSs. Depth scale compressed relative to length scale.

TABLE 2. Schedule and Constituents of PRD1 and Silica Colloid Deposition and Recovery Experiments[a]

injection	array	constituents	injectate concentration	uncontaminated C_0 6.4 m depth	contaminated C_0 8.7 m depth
deposition	1	PRD1	2.6×10^6 cpm L^{-1}	1.3×10^6 cpm L^{-1}	1.9×10^6 cpm L^{-1}
		SiO_2 colloids	500 mg L^{-1}	390 mg L^{-1}	470 mg L^{-1}
		NaBr	1.50 mM	0.79 mM	0.90 mM
	2	PRD1	2.1×10^6 cpm L^{-1}	1.5×10^6 cpm L^{-1}	1.8×10^6 cpm L^{-1}
		SiO_2 colloids	500 mg L^{-1}	400 mg L^{-1}	480 mg L^{-1}
		NaBr	1.50 mM	1.05 mM	1.12 mM
	3	PRD1	2.2×10^6 cpm L^{-1}	1.3×10^6 cpm L^{-1}	1.7×10^6 cpm L^{-1}
		SiO_2 colloids	500 mg L^{-1}	210 mg L^{-1}	310 mg L^{-1}
		NaBr	1.50 mM	0.90 mM	1.02 mM
recovery	1	NaOH	pH 12.5	pH 11.7	pH 11.8
		NaBr	1.50 mM	0.77 mM	1.04 mM
	2	NaDBS	5.7×10^{-4} M	5.2×10^{-4} M	5.2×10^{-4} M
		NaBr	1.50 mM	1.36 mM	1.07 mM
	3	ascorbic acid	1.82 mM	1.76 mM	2.09 mM
		NaBr	1.50 mM	0.86 mM	1.11 mM

[a] C_0 is the concentration measured in samples withdrawn immediately after injection. Each injection volume is 100 L.

contaminated groundwaters. When dilutions were required, groundwater from the same depth in the aquifer was used. Silica colloids were also examined by scanning electron microscopy (SEM; ISIS SX-30, 15 kV accelerating voltage). About 10 mL of high turbidity samples from each experiment was filtered onto 0.1 μm polycarbonate filters (VCTP, Millipore), dried at room temperature, mounted onto aluminum stubs, and gold-coated prior to SEM analysis.

Chemical Perturbations for Recovery. The release of PRD1 and silica colloids was promoted by injection of groundwater with elevated pH, anionic surfactant concentration, and reductant concentration (Table 2). Sodium hydroxide was added to the injectate after dissolution in 1 L of high purity water (Millipore Milli-Q) to achieve a pH of 12.5 in the injectate. Sodium dodecylbenzenesulfonate (NaDBS) was dissolved in 1 L of high purity water and added

to the groundwater injectate to achieve a concentration of 570 μM, about one-half of its critical micelle concentration (*39*), in the injectate. NaDBS concentration was measured using a methylene blue active substances (MBAS) test kit (Hach Co.) with a detection limit of 0.1 mg L^{-1}. l-Ascorbic acid was added to the groundwater injectate after dissolution in 1 L of high purity water to achieve a concentration of 1.82 mM. Ascorbate concentration was measured by UV spectrophotometry at λ = 264 nm (*40*). Calibrations were performed in both the uncontaminated and contaminated groundwater ($R^2 > 0.98$). Background absorbance at 264 nm for uncontaminated and contaminated groundwater was subtracted from the sample absorbance. Groundwater from the appropriate zone was used for dilutions.

Tracer. Bromide, added as sodium bromide at 1.5 mM concentration, was the conservative tracer (Table 2). Bromide concentration was measured using a bromide-specific electrode (Orion 9435BN), reference electrode (Orion 900100), and an Orion 250A meter. Error for replicate samples was less than 5% for these measurements. The detection limit for bromide was 5×10^{-6} M.

Virus and Colloid Surface Characteristics. The electrophoretic mobilities of PRD1 and silica colloids were determined by microelectrophoresis (Brookhaven, model ZetaPlus) as a function of pH in the uncontaminated groundwater and at near-ambient pH in the contaminated groundwater. The pH values reported for these groundwater samples were measured in the laboratory after 15 days of shipping and storage in sealed stainless steel canisters and sample handling in open air. Sodium bromide (1.5 mM) was added to simulate the injections, and hydrochloric acid was used to adjust pH over a range from pH 3.2 to the ambient pH. For this analysis, concentrated PRD1 stocks (roughly 10^{10} mL^{-1}) were purified by rate-zonal centrifugation and resuspended in uncontaminated and contaminated groundwater stored in ground glass-stoppered bottles at 4 °C. ζ potentials were calculated from the electrophoretic mobilities using the Smoluchowski equation (*41*).

Aquifer Grain Surface Characteristics. Streaming potentials of the aquifer grains were measured in both groundwaters by a streaming potential analyzer equipped with a cylindrical cell and Ag electrodes (Brookhaven, model BI-EKA). Aquifer sediments (10 mL) were wet-packed into the cylindrical cell with the appropriate groundwater. The soil−groundwater mixture was equilibrated by circulating groundwater through the cell for at least 10 min. For each aquifer sediment, six separate analyses were performed. The fluid flow direction through the cell was alternated between analyses to minimize hysteresis associated with charge buildup on the electrodes. Streaming potentials were converted to ζ potentials using the Helmholtz−Smoluchowski equation and the Fairbrother and Mastin approach (*42*, *43*).

Thin sections (30 μm × 2 × 2 cm) of aquifer sediments were prepared by impregnation with epoxy resin and carbon coating for electron microprobe (JEOL, model JXA-8600) and energy-dispersive X-ray (EDX) analysis of surface coatings. The area of surfaces covered by iron-containing coatings (which appeared as bright rims on the quartz grains) were estimated to the nearest 5% for 400 grains. The mineralogy of the fine-grained fraction of the sediments was examined by X-ray diffraction (XRD; Scintag, model XPH-105) using Cu Kα radiation at a speed of 2° 2θ min^{-1} through a range of 0−60° 2θ. The fine-grained fraction was isolated by sonication (80 W; 30 min) of the bulk sediment in deionized water, sedimentation for 10 min, filtration of the remaining suspension through 0.1 μm polycarbonate filters, and mounting of the filter on a glass slide.

Calculation of Attenuation, Collision Efficiency, Recovery, and Interaction Forces. The relative breakthrough (RB, %) of an injected constituent was calculated as the ratio of the time-integrated mass of the constituent relative to that of the conservative tracer (*6*). The attenuation (%) of an injected constituent is 100 − RB. Following the colloid filtration model of kinetically controlled irreversible attachment of colloids to collector grains (*5*), collision efficiencies (α) were calculated for pulse inputs of PRD1 and silica colloids with consideration of the effect of longitudinal dispersion (*6*)

$$\alpha = \frac{d[[1 - 2(\alpha_L/x_1)\ln \mathrm{RB}]^2 - 1]}{6(1-\theta)\eta_0\alpha_L} \quad (1)$$

and without longitudinal dispersion effects (as commonly calculated for column studies) (*12*)

$$\alpha = \frac{-2d \ln \mathrm{RB}}{3(1-\theta)\eta_0 x_1} \quad (2)$$

where d is the diameter of the porous media grains, x_1 is the distance from the injection point to the sampling point, η_0 is the single collector efficiency for favorable deposition, and α_L is the longitudinal dispersivity (*6*)

$$\alpha_L = \frac{x_1(\Delta t/t_{peak})^2}{16 \ln 2} \quad (3)$$

where Δt is the duration of the breakthrough for which $[Br^-] > {}^1/_2[Br^-]_{max}$, $[Br^-]_{max}$ is the peak bromide concentration, and t_{peak} is the time to peak bromide concentration. The single collector efficiency η_0 was calculated using only the convective-diffusion contribution (*12*) owing to the small size of PRD1 and silica colloids with an average grain diameter of 0.6 mm, a porosity of 0.39, and fluid velocities estimated from the time of peak bromide breakthrough. We assumed that the ^{32}P breakthrough curves represented the breakthrough of the intact infective and noninfective PRD1. We were not able to check this assumption (by rate-zonal centrifugation) owing to the low concentrations of ^{32}P that reached the down-gradient MLSs.

Fractional recoveries of virus and silica colloids following the chemical perturbations were estimated as the quantity of virus or colloid recovered during the second injection divided by the quantity of virus or colloid immobilized during the first injection (*31*). The amount immobilized over the between the injection MLS and the first down-gradient MLS was calculated as the difference between the amount injected and the amount appearing at the down-gradient MLS integrated over time. The amount of virus or colloid recovered during the second injection was calculated as the amount appearing at the down-gradient MLS integrated over time.

Collision efficiencies were predicted using the interaction force boundary layer (IFBL) approximation (*10*−*12*) and Derjaguin−Landau−Verwey−Overbeek (DLVO) theory (*44*, *45*). PRD1, silica colloid, and aquifer grain ζ potentials were used as surface potentials in these calculations. Ionic strengths of 2.0 and 5.5 mM (the ambient ionic strength plus 1.5 mM NaBr) were used for the uncontaminated and contaminated groundwaters, respectively. For the PRD1-grain interaction, a Hamaker constant of 7×10^{-21} J was selected from the range of the Hamaker constants calculated by Murray and Parks (*16*) for polio virus interaction with quartz and various metal oxides. For the silica colloid-grain interaction, a Hamaker constant of 2×10^{-20} J was selected from the range of Hamaker constants used for quartz−quartz and hematite−quartz interactions (*46*).

Results

Silica Colloid and PRD1 Surface Characteristics. In the uncontaminated groundwater amended with 1.5 mM sodium

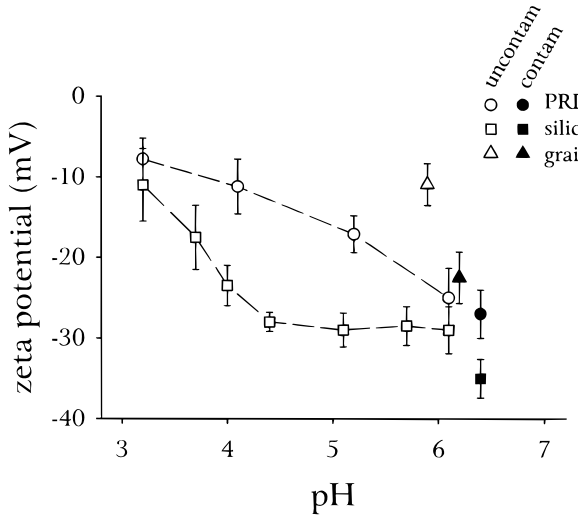

FIGURE 2. ζ potentials of PRD1, silica colloids, and uncontamina and contaminated aquifer grains in uncontaminated and conta nated groundwater as a function of pH. PRD1 and silica colloi potentials were measured by laser Doppler microelectrophore Grain ζ potentials were measured by streaming potential.

bromide, the ζ potentials of the PRD1 and silica collo were negative from pH 3.2 to the ambient pH of t uncontaminated groundwater (Figure 2). The mean potentials of the silica colloids were slightly more negat in the contaminated groundwater. The PRD1 ζ potenti were slightly more negative than those calculated from t electrophoretic mobilities of PRD1 in a calcium phosph buffer solution containing 10^{-4} M calcium (*7*).

Aquifer Grain Surface Characteristics. The ζ poten of contaminated sediments in contaminated groundwate more negative than that of the uncontaminated sedime in uncontaminated groundwater. The surfaces of the Ca Cod aquifer grains were 3.0 ± 10.0% coated by a mixture aluminum-, silicon-, iron-, and magnesium-containing pha in the uncontaminated zone and 3.5 ± 11.1% coated in t contaminated zone (Figure 3). A small fraction of the gra (about 10%) were partially coated (5 to 50% surface covera for each grain), but most of the grains (about 90%) w uncoated. This small amount of surface coverage agr well with the relatively low sediment Fe(III) concentratic removed by reductive extraction in the aquifer sedime (Table 1). Minerals in the fine-grained fraction of t sediments from both zones included quartz, feldspar, l olinite, illite/muscovite, and smectites. Crystalline forms ferric oxyhydroxide were not detected by XRD, suggest that amorphous forms of ferric oxyhydroxide may be t source of the ferric iron removed by reductive extracti Amorphous ferric oxyhydroxide phases were recently d tected in coatings on a quartz grain from a southern Atlan Coastal Plain sand (*47*).

PRD1 and Silica Colloid Deposition. PRD1 and silica colloids displayed measurable breakthroughs at the first down-gradient MLS (Figure 4a,b). Clear breakthrough curves were not detected further down-gradient (*48*). PRD1 and silica colloids were less attenuated in the contaminated zone than in the uncontaminated zone (Table 3). Collision efficiencies calculated with and without dispersion varied by up to a factor of 3.4. Values of collision efficiencies calculated with dispersion were always larger than the nondispersion values.

Silica Colloid and PRD1 Recovery During Chemical Perturbations. PRD1 and silica colloids were detected at the first down-gradient MLS during the chemical perturbations (Figures 5−7). Concentrations of PRD1 and silica

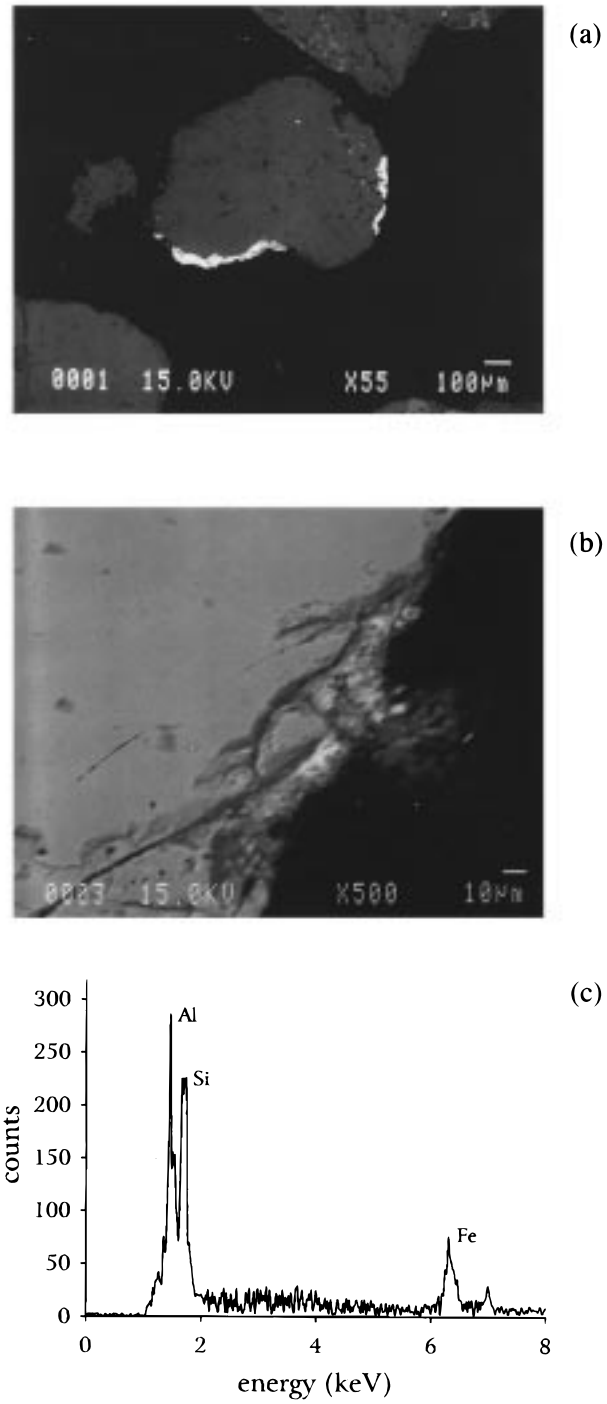

FIGURE 3. Electron microprobe images of thin section of contaminated zone sediments of the Cape Cod aquifer showing Al-, Si-, and Fe-rich coating on quartz grain at two different scales: (a) scale bar, 100 μm; magnification, 55 times; (b) scale bar, 10 μm, magnification 500 times; and (c) EDX scan of coating.

colloids detected further down-gradient were very low (*48*). The recoveries of PRD1 and silica colloids ranged from 0.5 to 240% (Table 4). During the elevated pH injection, silica colloid recoveries measured by UV absorbance exceeded 100% owing to mobilization of natural colloids (Figure 8). Unlike the elevated surfactant and reductant arrays, the elevated pH array was not subjected to a chemical perturbation to mobilize natural colloids prior to the deposition injection. On the basis of SEM examination, we estimated that about 60% of the mass of filtered particles originated from the injected silica colloids. Recalculation of the silica

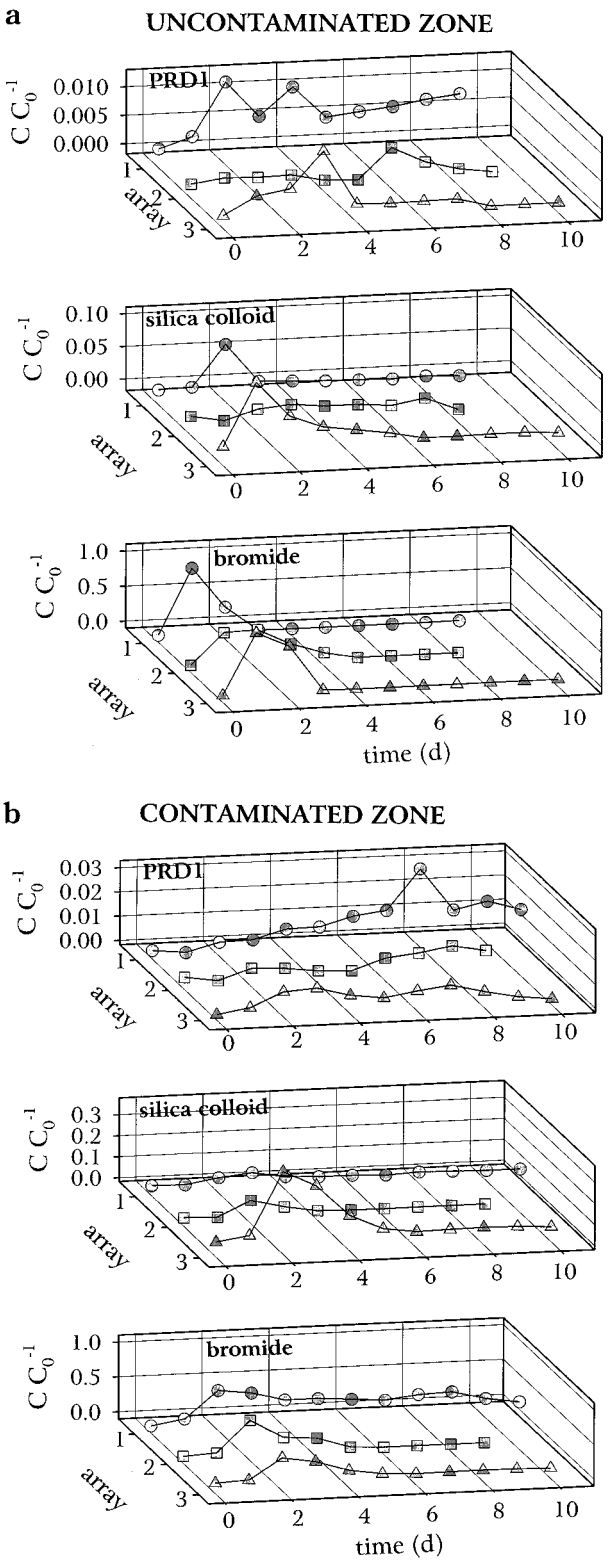

FIGURE 4. Breakthroughs of PRD1, silica colloids, and bromide at the 0.9 m transport distance in the (a) uncontaminated (6.4 m depth) and (b) contaminated (8.7 m depth) zones of array 1. Concentrations normalized by the concentration measured immediately after injection.

colloid recovery using 60% of the turbidity measurement for each sample resulted in maximum recoveries near 100%. For the arrays subjected to a prior chemical perturbation, SEM examination of filtered particles revealed at least 90% silica colloids.

Discussion

Silica Colloid and PRD1 ζ Potentials During Injections. The PRD1 pH_{pzc} in the uncontaminated groundwater is less than 3.2, slightly lower than the PRD1 pH_{pzc} of less than 4.5 in a calcium phosphate solution (*7*). Positive ζ potentials have not been measured for PRD1. On the basis of studies by Penrod et al. (*18*), these low pH_{pzc} values for PRD1 indicate that deprotonated carboxyl groups in amino acids dominate the surface speciation of the PRD1 protein capsid. For the silica colloids, the negative ζ potentials reflect the predominance of deprotonated surface hydroxyls at pH values above the pH_{pzc} value of about 2−2.5 reported for silica (*49*).

The silica colloid ζ potentials were slightly more negative in the contaminated groundwater, but no significant difference was observed between the PRD1 ζ potentials in the contaminated and uncontaminated groundwaters. For PRD1, a slightly more negative ζ potential was expected in the contaminated groundwater because of the slightly higher pH and higher concentration of organic matter in the contaminated groundwater. Previous studies have shown that surfactants (*50*) and fulvic acid (*51*) have produced more negative ζ potentials on viruses. The silica colloids, however, appear to have reached a constant ζ potential at about pH 4.4, so the more negative ζ potential measured in the contaminated groundwater cannot be attributed to the higher pH. The more negative ζ potential must be attributed to adsorption of either organic matter or phosphate. Extensive adsorption of humic substances to silica at pH near 6.0 is unlikely owing to electrostatic repulsion (*52*), but bivalent cations in the contaminated groundwater may enhance adsorption by reducing the negative charge of the humic substances.

Aquifer Grain ζ Potentials. The Cape Cod aquifer grains are composed of quartz, feldspar, and mica, all negatively charged minerals at the ambient pH of the groundwaters. The coatings are composed of clay minerals and amorphous ferric oxyhydroxides. Both clay minerals and ferric oxyhydroxides may be positively charged at the ambient pH (*49*). The ζ potentials measured for these grains with heterogeneous surfaces are negative, indicating that the positively charged patches must cover only a small fraction of the grain surfaces. Thus, these ζ potentials agree with the low patch surface coverage detected by microprobe/EDX. The ζ potential of the contaminated grains, where organic matter and phosphate are more abundant in both the groundwater and sediments, was more negative than that of the uncontaminated grains. Sufficient adsorption of organic matter and phosphate to the positively charged surfaces can mask the negative charge or even reverse the surface charge (*53*). The uncontaminated and contaminated zone sediments contain essentially the same minerals, the same amount of reducible iron, and the same coating surface coverages; therefore, we attribute the more negative ζ potential of the contaminated sediment to the differences in adsorbed organic matter and phosphate.

PRD1 and Silica Colloid Deposition Behavior. Most studies of virus attachment to mineral grains conclude that electrostatic forces dominate the interaction between virus and grain surfaces (*8, 16*−*19*) as they do for mineral colloid interactions with grains. If electrostatic forces dominated, then the measured ζ potentials should provide a qualitative explanation for the observed virus attachment behavior. The ζ potential data indicate that ferric oxyhydroxides and clay mineral edges in the Cape Cod sediments enhance PRD1 and silica colloid attachment and that organic matter in the sewage plume inhibits PRD1 and silica colloid attachment. Positively charged oxides limit virus and bacteria transport because "biocolloids" are typically negatively charged at the ambient pH of most waters and are electrostatically attracted

TABLE 3. Summary of Relative Breakthroughs (RB) and Collision Efficiencies (α) Calculated with and without Dispersion for PRD1 and Silica Colloids

	colloid	groundwater zone	RB (%)	ν_0	α with dispersion	α without dispersion
array 1	PRD1	uncontaminated	4.9	0.17	0.017	0.013
0.9 m distance		contaminated	4.5	0.24	0.0098	0.0097
	silica	uncontaminated	9.5	0.12	0.017	0.014
		contaminated	16	0.17	0.0089	0.0077
array 2	PRD1	uncontaminated	1.0	0.18	0.049	0.018
0.9 m distance		contaminated	6.0	0.22	0.018	0.0091
	silica	uncontaminated	9.7	0.13	0.020	0.013
		contaminated	35	0.16	0.0056	0.0047
array 3	PRD1	uncontaminated	1.5	0.16	0.029	0.018
1.0 m distance		contaminated	2.5	0.24	0.019	0.010
	silica	uncontaminated	19	0.11	0.033	0.0096
		contaminated	61	0.18	0.0022	0.0019
means and std dev for	PRD1	uncontaminated	2.5 ± 1.7		0.032 ± 0.016	0.016 ± 0.002
transport parameters		contaminated	4.3 ± 1.4		0.016 ± 0.005	0.0096 ± 0.0005
	silica	uncontaminated	13 ± 4		0.023 ± 0.009	0.012 ± 0.002
		contaminated	37 ± 16		0.0056 ± 0.0034	0.0048 ± 0.0029

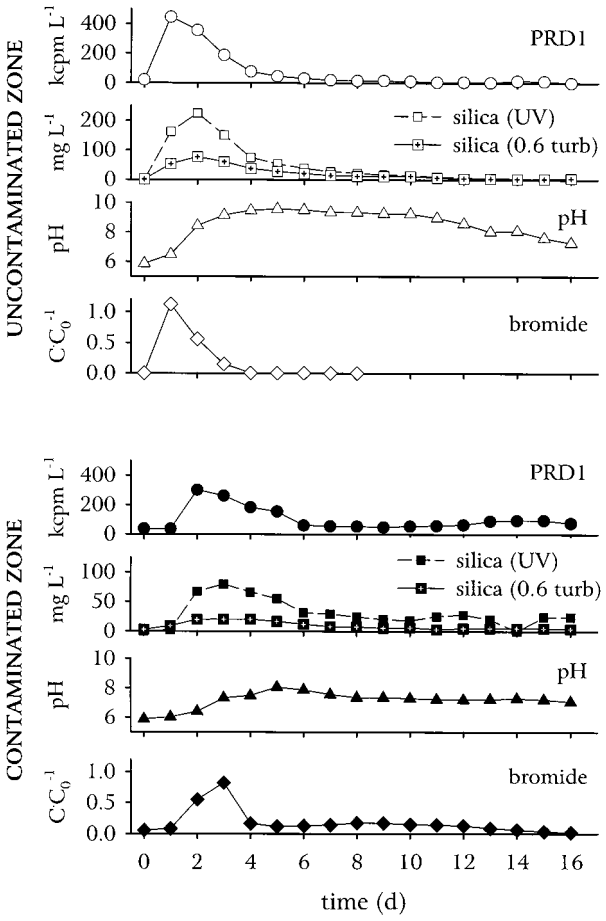

FIGURE 5. Release of PRD1 and silica colloids and breakthroughs of pH and bromide at the 0.9 m transport distance in the uncontaminated (6.4 m depth) and contaminated (8.7 m depth) zones of array 1 during the elevated pH recovery experiment. Silica colloid concentrations measured by ultraviolet absorption (UV) and turbidity and converted to mass concentrations. Turbidity measurement of silica colloid concentration decreased by a factor of 0.6 owing to presence of natural colloids mobilized by elevated pH.

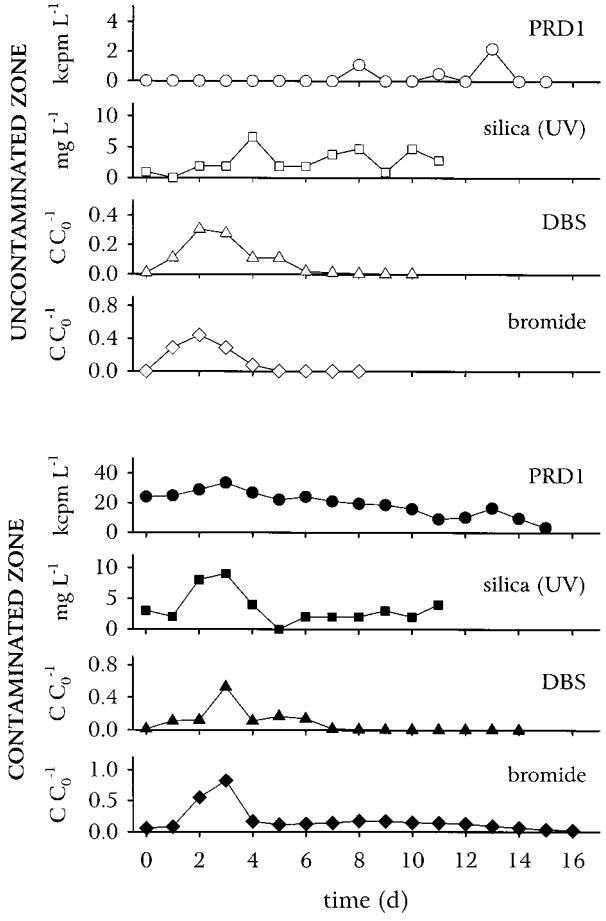

FIGURE 6. Release of PRD1 and silica colloids and breakthroughs of dodecylbenzenesulfonate (DBS) and bromide at the 0.9-m transport distance in the uncontaminated (6.4 m depth) and contaminated (8.7 m depth) zones of array 2 during the elevated surfactant recovery experiment. Silica colloid concentrations measured by ultraviolet absorption (UV).

to positively charged surfaces (*16, 17, 54−57*). Organic matter of natural and anthropogenic (e.g., sewage, surfactants) origin hinders virus attachment to mineral surfaces (*54, 58−64*), presumably by adsorbing to and masking virus attachment sites. Similarly, silica colloid transport depends on the fraction of grains coated by positively charged ferric oxide patches (*65*) and the transport of ferric oxide colloids through quartz sands is enhanced by natural organic matter (*66, 67*).

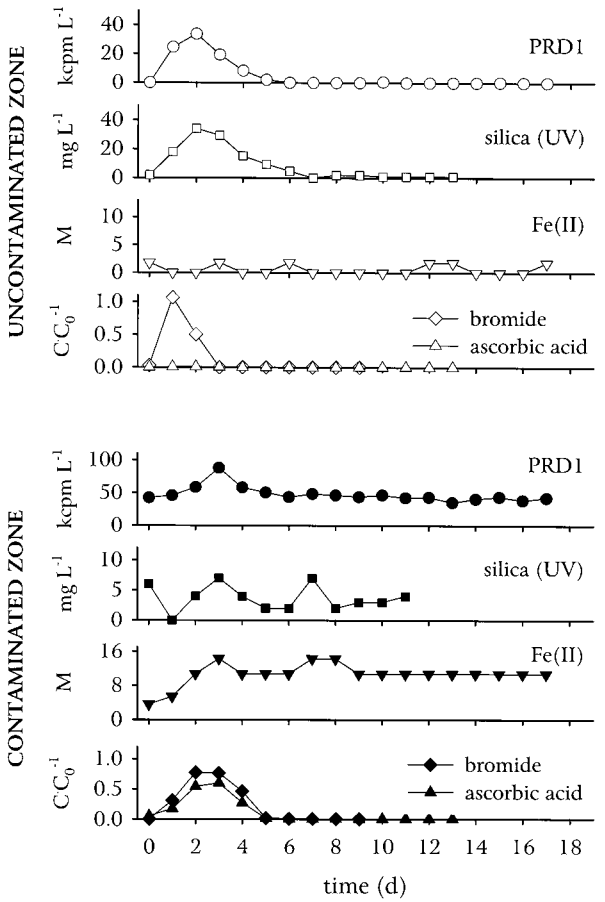

FIGURE 7. Release of PRD1, silica colloids, and ferrous iron and breakthroughs of ascorbic acid and bromide at the 1-m transport distance in the uncontaminated (6.4 m depth) and contaminated (8.7 m depth) zones of array 3 during the elevated reductant recovery experiment. Silica colloid concentrations measured by ultraviolet absorption (UV).

TABLE 4. Recovery of PRD1 and Silica Colloids over the First Meter of Transport[a]

array	colloid	groundwater zone	recovery (%)
1 elevated pH NaOH	PRD1	uncontaminated	100 ± 11
		contaminated	78 ± 10
	silica (UV)	uncontaminated	240 ± 18
		contaminated	120 ± 11
	silica (0.6 turb)	uncontaminated	103 ± 9
		contaminated	37 ± 5
2 elevated surfactant NaDBS	PRD1	uncontaminated	0.5 ± 5.5
		contaminated	49 ± 7
	silica (UV)	uncontaminated	3.5 ± 6.1
		contaminated	15 ± 5
3 elevated reductant ascorbic acid	PRD1	uncontaminated	3.8 ± 6.7
		contaminated	24 ± 4
	silica (UV)	uncontaminated	51 ± 6
		contaminated	27 ± 4

[a] Two pairs of recoveries are listed for the silica colloids in array 1. The first pair is for silica colloids measured by UV absorbance. The second pair is for silica colloids measured as 0.6 times the sample turbidity to account for natural colloids.

Relating Collision Efficiencies to Electrostatic Interactions. Using the interaction force boundary layer approximation and DLVO theory, we can predict collision efficiencies for the PRD1 and silica colloid interactions with the aquifer grains (Figure 9). The predicted collision efficiencies follow the trend of the measured collision efficiencies—they increase as the ζ potentials of the PRD1, silica, and grains become less negative. However, the predicted and measured collision efficiencies deviate greatly. The predicted collision efficiencies are extremely sensitive to variations in the interaction energy barrier size, which depends on the ζ potentials of the interacting surfaces, owing to the Arrhenius-type relationship between the collision efficiency and energy barrier size, a phenomenon long noted in studies of colloid deposition (*12*). Despite the lack of a one-to-one correspondence of the predicted and measured collision efficiencies, the modest but significant increase in the collision efficiencies that occurs as ζ potentials become less negative indicates that electrostatic forces dominate the attachment of PRD1 and silica to these aquifer grains. It should be noted that the IFBL analysis is not valid for chemically heterogeneous grain surfaces. A more appropriate analysis should consider the role of aquifer grain geochemical heterogeneities.

Grain Surface Heterogeneity and Collision Efficiencies. At the ambient pH of the groundwaters, the negatively charged PRD1 would be effectively collected by positively

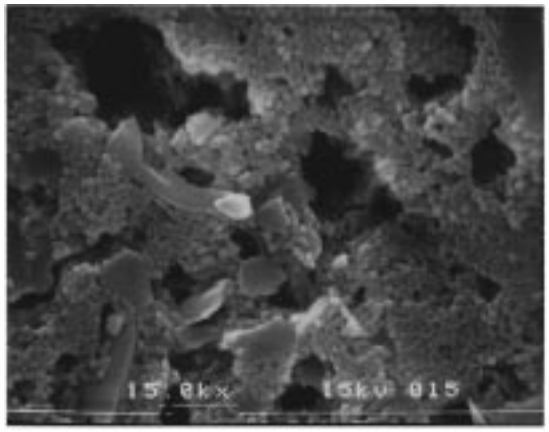

FIGURE 8. Scanning electron microscope image of colloids trapped on a 0.1 μm filter after filtration of about 9 mL of groundwater during the elevated pH recovery experiment showing natural colloids and silica colloids (spherical, about 100 nm diameter). The natural colloids included kaolinite, smectites, illite/muscovite, quartz, and feldspar (*48*). Scale bar (second elevated dash, below magnification) is 1 μm and magnification is 15 000 times.

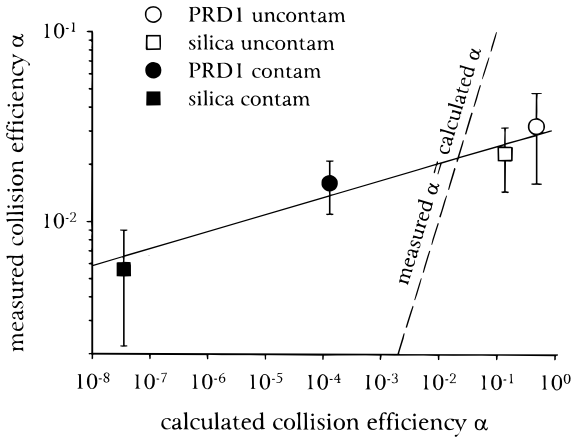

FIGURE 9. Measured versus predicted collision efficiencies for the PRD1 and silica colloid injection. Collision efficiencies predicted using the interaction force boundary layer approximation and DLVO theory.

charged surfaces of the ferric oxyhydroxides and clay edges and repelled by the negatively charged quartz surfaces (*17*). The apparent collision efficiency, $\alpha_{apparent}$, the value calculated with data from the field experiments (Table 3), should reflect the summed contributions of colloid interaction with the positively charged patches and the underlying negatively charged surface (*14, 65*). For PRD1 interaction with the positively charged patches, we can assume that $\alpha_{patch} \approx 1$ owing to electrostatic attraction. For PRD1 interaction with quartz surfaces, we can assume that $\alpha_{qtz} \approx 6 \times 10^{-3}$, a collision efficiency calculated for PRD1 deposition on glass beads (*7*). With the microprobe/EDX estimates of patch surface coverage, f_{patch}, we can estimate the overall collision efficiencies using the following equation (*14*):

$$\alpha_{apparent} = f_{patch}\alpha_{patch} + (1 - f_{patch})\alpha_{qtz} \quad (6)$$

With $f_{patch} = 0.030$ in the uncontaminated zone, eq 6 predicts $\alpha_{apparent} = 0.036$, a fairly close match to the measured mean collision efficiency of 0.032 for PRD1. With $f_{patch} = 0.035$ in the contaminated zone, $\alpha_{apparent} = 0.041$, a prediction about 2.5 times greater than the measured mean collision efficiency of 0.016. The discrepancy between the predicted and measured collision efficiency in the contaminated zone suggests that only about 40% of the patch surface area is effectively collecting PRD1 in the contaminated zone. It is reasonable to assume that adsorption of organic matter has blocked PRD1 deposition on the remaining 60% of the positively charged patches.

According to Coston et al. (*33*), measurement of the surface coverage of patches depends on the technique used to detect the coatings. Scanning electron microscopy and EDX detected only patchy coatings of greater than 5 μm thickness. Time-of-flight-secondary ion mass spectroscopy detected the universal presence of 10 nm-thick layers of iron on grain surfaces, even on those for which the visible iron staining had been removed by hydroxylamine hydrochloride extraction. The close agreement between the predicted and measured collision efficiencies in the uncontaminated zone suggest that the resolution afforded by the microprobe/EDX analysis provides a good estimate of the extent of surface coverage affecting PRD1 and silica colloid deposition.

PRD1 and Silica Colloid Release by Elevated pH. The NaOH injection was designed to reverse the charge on the ferric oxyhydroxide coatings by raising pH above the pH_{iep} of ferric oxyhydroxides (*49*). Although the precision of the silica colloid recovery measurement is clouded by the presence of the natural colloids, it appears that similar amounts of PRD1 and silica colloids were released and that release occurred more readily in the uncontaminated zone. In the uncontaminated zone, the lack of buffering in the groundwater and sediments resulted in a greater increase in pH and greater release of PRD1 and silica colloids than in the contaminated zone. The pH in the uncontaminated zone peaked at nearly 10 at the 1 m distance (injection pH 11.7), while the pH in the contaminated zone peaked at only 8.5 at the 1 m distance (injection pH 11.5). An increase of pH to 10 is sufficient to reverse the surface charge of any ferric oxyhydroxide, but an increase to pH 8.5 may not exceed the pH_{iep} of some ferric oxyhydroxides. The greater release of PRD1 and silica colloids in the uncontaminated zone must be attributed to the increase in pH well in excess of the pH_{iep} of the ferric oxyhydroxide coatings.

In the contaminated zone of the Cape Cod aquifer, Bales et al. (*24*) found that injection of a pH 8.3 solution containing an unspecified concentration of phosphate for buffering effectively remobilized PRD1 (a fractional recovery was not measured). This injection caused the detachment of PRD1 even when the pH increase down-gradient of the injection was only slightly above the ambient pH. It is likely that the phosphate augmented the charge reversal caused by the pH increase by adsorbing to the ferric oxyhydroxide coatings.

PRD1 and Silica Colloid Release by Anionic Surfactant Addition. Dodecylbenzenesulfonate (DBS) was added to alter the ferric oxyhydroxide surface charge and promote release. DBS is an anionic surfactant that readily adsorbs to positively charged oxide surfaces and reverses surface charge by hemimicelle formation (*68*). Similar surfactants have been shown to mobilize natural colloids (*69*) and cause permeability reduction through colloid mobilization (*70*). The high DBS injection concentration made it difficult to determine with any precision the amount of DBS lost to aquifer sediments by adsorption. Only a small fraction of the DBS injected would be required to saturate the ferric oxyhydroxide surfaces with adsorbed DBS (*31*); however, DBS was much less effective at mobilizing PRD1 and silica colloids than the increase in pH. Similarly, Bales et al. (*7*) showed that 1% Tween 80 and 2.5% beef extract solutions were only marginally effective at mobilizing PRD1 and MS2, another bacteriophage, relative to an increase in pH to 8 in a sodium phosphate solution. Bales et al. (*7*) speculated that the high ionic strength of the surfactant and beef extract solutions inhibited virus detachment. Our addition of DBS to the Cape Cod groundwater caused an increase in ionic strength (0.6 mM) less than that caused by the sodium bromide tracer (about 1.5 mM).

DBS was much more effective at mobilizing PRD1 and silica colloids in the contaminated zone. In a previous experiment, Pieper et al. (*31*) similarly observed that a 25 mg L^{-1} mixture of linear alkylbenzenesulfonates (LAS) recovered 87% of the injected PRD1 in the contaminated zone and only 2% in the uncontaminated zone. The abundance of organic matter in the contaminated zone must reduce the amount of surfactant needed to reverse the charge of ferric oxyhydroxide surfaces. In this experiment, the higher concentration of DBS (200 mg L^{-1}) did not improve recovery. The results suggest that PRD1 and silica colloids are more strongly bound in the uncontaminated zone.

PRD1 and Silica Colloid Release by Reductant Addition. Ascorbic acid was added to remove the ferric oxyhydroxide coatings by reductive dissolution, resulting in the release of PRD1 and silica colloids attached to the coatings. Ryan and Gschwend (*69*) observed that reductive dissolution by ascorbate mobilized natural colloids from a similar ferric oxyhydroxide-coated quartz sand as long as increases in the ascorbate concentration did not raise ionic strength to a level too high to inhibit release. In this experiment, ascorbic acid addition promoted PRD1 and silica colloid release that was somewhat comparable to the surfactant addition but less than that caused by the pH increase. The amount of ascorbic acid injected in this experiment was similar to the amount promoting the maximum colloid release in the experiments of Ryan and Gschwend (*69*).

The amount of PRD1 and silica colloid release varied inconsistently in these experiments. Ascorbic acid appeared to be effectively dissolving ferric oxyhydroxides in the contaminated zone because the Fe(II) concentration increased as the ascorbic acid broke through; however, Fe(II) release continued near the peak level of Fe(II) release for 15 days beyond the ascorbic acid breakthrough. In contrast, very little ascorbic acid broke through, and very little Fe(II) was released in the uncontaminated zone. Some ascorbic acid may have been oxidized by oxygen, although no significant changes in the oxygen content were observed. Released Fe(II) may have been readsorbed by aquifer grains or by released colloids, in which case the Fe(II) would promote destabilization and deposition. Based on these results, it is difficult to assess the dependence of PRD1 and silica colloid recovery by ascorbic acid addition. However, the effect of ascorbic acid does serve to emphasize the importance of

ferric oxyhydroxide-containing patches on the transport of PRD1 and silica colloids in the Cape Cod aquifer.

Acknowledgments

This research was funded by a cooperative agreement (CR824593-01) with the R. S. Kerr Laboratory of the U.S. Environmental Protection Agency (EPA) and the National Science Foundation (EAR-9418472). We thank Bob Puls (EPA) for project guidance, Denis LeBlanc, Kathy Hess, and Tim McCobb of the U.S. Geological Survey, Massachusetts District, for access to the field site and collection of sediment and groundwater samples, Mike Bonewitz for field work, Jon Loveland for virus preparation, Dave Metge, Jon Larson, and Dean Abadzic for data analysis, Robin Magelky for electrophoretic mobility measurements, John Drexler for scanning electron microscopy, and two anonymous reviewers for insightful comments.

Literature Cited

(1) Macler, B. A. *J. Am. Water Works Assoc.* **1996**, *88*, 47−55.
(2) Yates, M. V. *J. Am. Water Works Assoc.* **1995**, *87*, 76−85.
(3) Yates, M. V.; Yates, S. R.; Wagner, J.; Gerba, C. P. *J. Contam. Hydrol.* **1987**, *1*, 329−345.
(4) Park, N.-S.; Blandford, T. N.; Wu, Y.-S.; Huyakorn, P. S. CANVAS: A composite analytical-numerical model for viral and solute transport simulation. Documentation and user's guide, Version 1.0.; HydroGeoLogic, Inc.: Herndon, VA, 1993.
(5) Yao, K.-M.; Habibian, M. T.; O'Melia, C. R. *Environ. Sci. Technol.* **1971**, *5*, 1105−1112.
(6) Harvey, R. W.; Garabedian, S. P. *Environ. Sci. Technol.* **1991**, *25*, 178−185.
(7) Bales, R. C.; Hinkle, S. R.; Kroeger, T. W.; Stocking, K.; Gerba, C. P. *Environ. Sci. Technol.* **1991**, *25*, 2088−2095.
(8) Gerba, C. P. *Adv. Appl. Microbiol.* **1984**, *30*, 133−169.
(9) Ryan, J. N.; Elimelech, M. *Colloids Surf. A* **1996**, *107*, 1−56.
(10) Ruckenstein, E.; Prieve, D. C. *J. Chem. Soc., Faraday Trans. 2* **1973**, *69*, 1522−1536.
(11) Spielman, L. A.; Friedlander, S. K. *J. Colloid Interface Sci.* **1974**, *46*, 22−31.
(12) Elimelech, M.; Gregory, J.; Jia, X.; Williams, R. *Particle Deposition & Aggregation. Measurement, Modelling, and Simulation*; Butterworth-Heinemann: Oxford, England, 1995.
(13) Elimelech, M.; O'Melia, C. R. *Environ. Sci. Technol.* **1990**, *24*, 1528−1536.
(14) Song, L.; Johnson, P. R.; Elimelech, M. *Environ. Sci. Technol.* **1994**, *28*, 1164−1171.
(15) Litton, G. M.; Olson, T. M. *J. Colloid Interface Sci.* **1994**, *165*, 522−525.
(16) Murray, J. P.; Parks, G. A. In *Particulates in Water. Characterization, Fate, Effects, and Removal*; Kavanaugh, M. C., Leckie, J. O., Eds.; American Chemical Society: Washington, DC, 1980; pp 97−133.
(17) Loveland, J. P.; Ryan, J. N.; Amy, G. L.; Harvey, R. W. *Colloids Surf. A* **1996**, *107*, 205−221.
(18) Penrod, S. L.; Olson, T. M.; Grant, S. B. *Langmuir* **1996**, *12*, 5576−5587.
(19) Redman, J. A.; Grant, S. B.; Olson, T. M.; Hardy, M. E.; Estes, M. K. *Environ. Sci. Technol.* **1997**, *31*, 3378−3383.
(20) Bales, R. C.; Li, S.; Maguire, K. M.; Yahya, M. T.; Gerba, C. P. *Water Resour. Res.* **1993**, *29*, 957−963.
(21) Kinoshita, T.; Bales, R. C.; Maguire, K. M.; Gerba, C. P. *J. Contam. Hydrol.* **1993**, *14*, 55−70.
(22) Harvey, R. W.; George, L. H.; Smith, R. L.; LeBlanc, D. R. *Environ. Sci. Technol.* **1989**, *23*, 51−56.
(23) Harvey, R. W.; Kinner, N. E.; Bunn, A.; MacDonald, D.; Metge, D. *Appl. Environ. Microbiol.* **1995**, *61*, 209−217.
(24) Bales, R. C.; Li, S.; Maguire, K. M.; Yahya, M. T.; Gerba, C. P.; Harvey, R. W. *Ground Water* **1995**, *33*, 653−661.
(25) Bales, R. C.; Li, S.; Yeh, T.-C. J.; Lenczewski, M. E.; Gerba, C. P. *Water Resour. Res.* **1997**, *33*, 639−648.
(26) LeBlanc, D. R. Water-Supply Paper 2218, U.S. Geological Survey: 1984; 28 pp.
(27) Hess, K. H.; Wolf, S. H.; Celia, M. A. *Water Resour. Res.* **1992**, *28*, 2011−2027.
(28) Kent, D. B.; Davis, J. A.; Anderson, L. C. D.; Rea, B. A.; Waite, T. D. *Water Resour. Res.* **1994**, *30*, 1099−1114.
(29) Smith, R. L.; Howes, B. L.; Garabedian, S. P. *Appl. Environ. Microbiol.* **1991**, *57*, 1997−2004.
(30) Barber, L. B. I.; Thurman, E. M.; Schroeder, M. P.; LeBlanc, D. R. *Environ. Sci. Technol.* **1988**, *22*, 205−211.
(31) Pieper, A. P.; Ryan, J. N.; Harvey, R. W.; Amy, G. L.; Illangasekare, T. H.; Metge, D. W. *Environ. Sci. Technol.* **1997**, *31*, 1163−1170.
(32) LeBlanc, D. R.; Garabedian, S. P.; Hess, K. H.; Gelhar, L. W.; Quadri, R. D.; Stollenwerk, K. G.; Wood, W. W. *Water Resour. Res.* **1991**, *27*, 895−910.
(33) Coston, J. A.; Fuller, C. C.; Davis, J. A. *Geochim. Cosmochim. Acta* **1995**, *59*, 3535−3547.
(34) Olsen, R. H.; Siak, J.-S.; Gray, R. H. *J. Virology* **1974**, *14*, 689−699.
(35) IAWPRC Study Group on Health Related Water Microbiology. *Water Res.* **1991**, *25*, 529.
(36) Davis, T. N.; Muller, E. D.; Cronan, J. E., Jr. *Virology* **1982**, *126*, 600−613.
(37) Yahya, M. T.; Galsomies, L.; Gerba, C. P.; Bales, R. C. *Water Sci. Technol.* **1993**, *27*, 409−412.
(38) Murray, J. P.; Laband, S. J. *Appl. Environ. Microbiol.* **1979**, *37*, 480−486.
(39) Mukerjee, P.; Mysels, K. J. Report NSRDS-NBS 36, National Bureau of Standards, Washington, DC, 1971; 227 pp.
(40) Banwart, S.; Davies, S.; Stumm, W. *Colloids Surf.* **1989**, *39*, 303−309.
(41) Hunter, R. J. *Zeta Potential in Colloid Science: Principles and Applications*; Academic Press: London, 1981.
(42) Fairbrother, F.; Mastin, H. *J. Chem. Soc.* **1924**, *125*, 2319−2330.
(43) Elimelech, M.; Chen, W. H.; Waypa, J. J. *Desal.* **1994**, *95*, 269−286.
(44) Derjaguin, B. V.; Landau, L. *Acta Physicochim. URSS* **1941**, *14*, 633−662.
(45) Verwey, E. J. W.; Overbeek, J. Th. G. *Theory of the Stability of Lyophobic Colloids*; Elsevier: Amsterdam, 1948.
(46) Israelachvili, J. *Intermolecular and Surface Forces*; Academic Press: London, 1992.
(47) Swartz, C. H.; Ulery, A. L.; Gschwend, P. M. *Geochim. Cosmochim. Acta* **1997**, *61*, 707−718.
(48) Ard, R. A. Natural and artificial colloid mobilization in a sewage-contaminated aquifer: Field and laboratory experiments. M.S. Thesis, University of Colorado at Boulder, 1997.
(49) Parks, G. A. In *Equilibrium Concepts in Natural Water Systems*; Stumm, W., Ed.: American Chemical Society: Washington, DC, 1967; pp 121−160.
(50) Small, D. A.; Moore, N. F. *Appl. Environ. Microbiol.* **1987**, *53*, 598−602.
(51) Bixby, R. L.; O'Brien, D. J. *Appl. Environ. Microbiol.* **1979**, *38*, 840−845.
(52) Davis, J. A. *Geochim. Cosmochim. Acta* **1982**, *46*, 2381−2393.
(53) Liang, L.; Morgan, J. J. *Aquatic Sci.* **1990**, *52*, 32−55.
(54) Moore, R. S.; Taylor, D. H.; Sturman, L. S.; Reddy, M. M.; Fuhs, G. W. *Appl. Environ. Microbiol.* **1981**, *42*, 963−975.
(55) Farrah, S. R.; Preston, D. R. *Water Sci. Technol.* **1991**, *24*, 235−240.
(56) Scholl, M. A.; Harvey, R. W. *Environ. Sci. Technol.* **1992**, *26*, 1410−1417.
(57) Mills, A. L.; Herman, J. S.; Hornberger, G. M.; DeJesús, T. H. *Appl. Environ. Microbiol.* **1994**, *60*, 3300−3306.
(58) Charney, J.; Machlowitz, R. A.; Spicer, D. S. *Virology* **1962**, *18*, 495−497.
(59) Burge, W. D.; Enkiri, N. K. *J. Environ. Qual.* **1978**, *7*, 73−76.
(60) Sobsey, M. D.; Dean, C. H.; Knuckles, M. E.; Wagner, R. A. *Appl. Environ. Microbiol.* **1980**, *40*, 92−101.
(61) Gerba, C. P.; Goyal, S. M.; Cech, I.; Bogdan, G. F. *Environ. Sci. Technol.* **1981**, *15*, 940−944.
(62) Moore, R. S.; Taylor, D. H.; Reddy, M. M. M.; Sturman, L. S. *Appl. Environ. Microbiol.* **1982**, *44*, 852−859.
(63) Atherton, J. G.; Bell, S. S. *Water Res.* **1983**, *17*, 943−948.
(64) Fuhs, G. W.; Chen, M.; Sturman, L. S.; Moore, R. S. *Microb. Ecol.* **1985**, *11*, 25−39.
(65) Johnson, P. R.; Sun, N.; Elimelech, M. *Environ. Sci. Technol.* **1996**, *30*, 3284−3293.
(66) Amirbahman, A.; Olson, T. M. *Environ. Sci. Technol.* **1993**, *27*, 2807−2813.
(67) Kretzschmar, R.; Robarge, W. P.; Amoozegar, A. *Water Resour. Res.* **1995**, *31*, 435−445.
(68) Dick, S. G.; Fuerstenau, D. W.; Healy, T. W. *J. Colloid Interface Sci.* **1971**, *37*, 595−602.
(69) Ryan, J. N.; Gschwend, P. M. *Environ. Sci. Technol.* **1994**, *28*, 1717−1726.
(70) Allred, B.; Brown, G. O. *Ground Water Monit. Remed.* **1994**, 174−184.

(71) Walter, D. A.; Rea, B. A.; Stollenwerk, K. G.; Savoie, J. Water-Supply Paper 2463, U.S. Geological Survey, 1996; 89 pp.
(72) Barber, L. B., II. Geochemical heterogeneity in a glacial outwash aquifer: Effect of particle size and mineralogy on sorption of nonionic organic solutes. Ph.D. Thesis, University of Colorado at Boulder, 1990.
(73) Ryan, J. N.; Gschwend, P. M. *Clays Clay Min.* **1991**, *39*, 509−518.

Received for review April 7, 1998. Revised manuscript received September 2, 1998. Accepted September 21, 1998.

ES980350+